Discovery of biased orientation of human DNA motif sequences affecting enhancer-promoter interactions and transcription of genes

Naoki Osato[1*]

[1]Department of Bioinformatic Engineering, Graduate School of Information Science and Technology, Osaka University, Osaka 565-0871, Japan

[*]Corresponding author

E-mail address: naokiosato11@gmail.com, nosato@ist.osaka-u.ac.jp

Abstract

Chromatin interactions have important roles for enhancer-promoter interactions (EPI) and regulating the transcription of genes. CTCF and cohesin proteins are located at the anchors of chromatin interactions, forming their loop structures. CTCF has insulator function limiting the activity of enhancers into the loops. DNA binding sequences of CTCF indicate their orientation bias at chromatin interaction anchors – forward-reverse (FR) orientation is frequently observed. DNA binding sequences of CTCF were found in open chromatin regions at about 40% - 80% of chromatin interaction anchors in Hi-C and in situ Hi-C experimental data. It has been reported that long range of chromatin interactions tends to include less CTCF at their anchors. It is still unclear what proteins are associated with chromatin interactions.

To find DNA binding motif sequences of transcription factors (TF), such as CTCF, and repeat DNA sequences affecting the interaction between enhancers and promoters of genes and their expression, first I predicted TF bound in enhancers and promoters using DNA motif sequences of TF and experimental data of open chromatin regions in monocytes and other cell types, which were obtained from public and commercial databases. Second, transcriptional target genes of each TF were predicted based on enhancer-promoter association (EPA). EPA was shortened at the genomic locations of FR or reverse-forward (RF) orientation of DNA motif sequence of a TF, which were supposed to be at chromatin interaction anchors and acted as insulator sites like CTCF.

The expression levels of the transcriptional target genes predicted based on the EPA were compared with those predicted from only promoters. Total 287 biased

orientation of DNA motifs (159 FR and 153 RF orientation, the reverse complement sequences of some DNA motifs were also registered in databases, so the total number was smaller than the number of FR and RF) affected the expression level of putative transcriptional target genes significantly in $CD14^+$ monocytes of four people in common. The same analysis was conducted in $CD4^+$ T cells of four people. DNA motif sequences of CTCF, cohesin and other transcription factors involved in chromatin interactions were found to be a biased orientation. Transposon sequences, which are known to be involved in insulators and enhancers, showed a biased orientation. The biased orientation of DNA motif sequences tended to be co-localized in the same open chromatin regions. Moreover, for ~85% of FR and RF orientations of DNA motif sequences, EPI predicted from EPA that were shortened at the genomic locations of the biased orientation of DNA motif sequence were overlapped with chromatin interaction data (Hi-C and HiChIP) significantly more than other types of EPAs.

Keywords: transcriptional target genes, gene expression, transcription factors, enhancer, enhancer-promoter interactions, chromatin interactions, CTCF, cohesin, open chromatin regions

Background

Chromatin interactions have important roles for enhancer-promoter interactions (EPI) and regulating the transcription of genes. CTCF and cohesin proteins are located at the anchors of chromatin interactions, forming their loop structures. CTCF has

55 insulator function limiting the activity of enhancers into the loops (Fig. 1A). DNA
56 binding sequences of CTCF indicate their orientation bias at chromatin interaction
57 anchors – forward-reverse (FR) orientation is frequently observed (de Wit et al. 2015;
58 Guo et al. 2015). About 40% - 80% of chromatin interaction anchors of Hi-C and in situ
59 Hi-C experiments include DNA binding motif sequences of CTCF. However, it has been
60 reported that long range of chromatin interactions tends to include less CTCF at their
61 anchors (Jeong et al. 2017). Other DNA binding proteins such as ZNF143, YY1, and
62 SMARCA4 (BRG1) are found to be associated with chromatin interactions and EPI
63 (Bailey et al. 2015; Barutcu et al. 2016; Weintraub et al. 2017). CTCF, cohesin, ZNF143,
64 YY1 and SMARCA4 have other biological functions as well as chromatin interactions
65 and EPI. The DNA binding motif sequences of the transcription factors (TF) are found
66 in open chromatin regions near transcriptional start sites (TSS) as well as chromatin
67 interaction anchors.

68 DNA binding motif sequence of ZNF143 was enriched at both chromatin
69 interaction anchors. ZNF143's correlation with the CTCF-cohesin cluster relies on its
70 weakest binding sites, found primarily at distal regulatory elements defined by the
71 'CTCF-rich' chromatin state. The strongest ZNF143-binding sites map to promoters
72 bound by RNA polymerase II (POL2) and other promoter-associated factors, such as the
73 TATA-binding protein (TBP) and the TBP-associated protein, together forming a
74 'promoter' cluster (Bailey et al. 2015).

75 DNA binding motif sequence of YY1 does not seem to be enriched at both
76 chromatin interaction anchors (Z-score < 2), whereas DNA binding motif sequence of

77 ZNF143 is significantly enriched (Z-score > 7; Bailey et al. 2015 Figure 2a). In the
78 analysis of YY1, to identify a protein factor that might contribute to EPI, (Ji et al. 2015)
79 performed chromatin immune precipitation with mass spectrometry (ChIP-MS), using
80 antibodies directed toward histones with modifications characteristic of enhancer and
81 promoter chromatin (H3K27ac and H3K4me3, respectively). Of 26 transcription factors
82 that occupy both enhancers and promoters, four are essential based on a CRISPR
83 cell-essentiality screen and two (CTCF, YY1) are expressed in >90% of tissues
84 examined (Weintraub et al. 2017). These analyses started from the analysis of histone
85 modifications of enhancer and promote marks rather than chromatin interactions. Other
86 protein factors associated with chromatin interactions may be found from other
87 researches.

88 As computational approaches, machine-learning analyses to predict chromatin
89 interactions have been proposed (Schreiber et al. 2017; Zhang et al. 2017). However,
90 they were not intended to find DNA motif sequences of TF affecting chromatin
91 interactions, EPI, and the expression level of transcriptional target genes, which were
92 examined in this study.

93 DNA binding proteins involved in chromatin interactions are supposed to affect
94 the transcription of genes in the loops formed by chromatin interactions. In my previous
95 analysis, the expression level of human putative transcriptional target genes was
96 affected, according to the criteria of enhancer-promoter association (EPA) (Fig. 1B;
97 (Osato 2018)). EPI were predicted based on EPA shortened at the genomic locations of
98 FR orientation of CTCF binding sites, and transcriptional target genes of each TF bound

99 in enhancers and promoters were predicted based on the EPI. The EPA affected the
100 expression levels of putative transcriptional target genes the most among three types of
101 EPA, compared with the expression levels of transcriptional target genes predicted from
102 only promoters (Fig. 2). The expression levels tended to be increased in monocytes and
103 $CD4^+$ T cells, implying that enhancers activated the transcription of genes, and
104 decreased in ES and iPS cells, implying that enhancers repressed the transcription of
105 genes. These analyses suggested that enhancers affected the transcription of genes
106 significantly, when EPI were predicted properly. Other DNA binding proteins involved
107 in chromatin interactions, as well as CTCF, may locate at chromatin interaction anchors
108 with a pair of biased orientation of DNA binding motif sequences, affecting the
109 expression level of putative transcriptional target genes in the loops formed by the
110 chromatin interactions. As experimental issues of the analyses of chromatin interactions,
111 chromatin interaction data are changed, according to experimental techniques, depth of
112 DNA sequencing, and even replication sets of the same cell type. Chromatin interaction
113 data may not be saturated enough to cover all chromatin interactions. Supposing these
114 characters of DNA binding proteins associated with chromatin interactions and avoiding
115 experimental issues of the analyses of chromatin interactions, here I searched for DNA
116 motif sequences of TF and repeat DNA sequences, affecting EPI and the expression
117 level of putative transcriptional target genes in $CD14^+$ monocytes and $CD4^+$ T cells of
118 four people and other cell types without using chromatin interaction data. Then, putative
119 EPI were compared with chromatin interaction data.
120

121 # Results

122 **Search for biased orientation of DNA motif sequences**

123 Transcription factor binding sites (TFBS) were predicted using open chromatin
124 regions and DNA motif sequences of transcription factors (TF) collected from various
125 databases and journal papers (see Methods). Transcriptional target genes were predicted
126 using TFBS in promoters and enhancer-promoter association (EPA) shortened at the
127 genomic locations of DNA binding motif sequence of a TF acting as insulator such as
128 CTCF and cohesin (RAD21 and SMC3) (Fig. 1B). To find DNA motif sequences of TF
129 acting as insulator, other than CTCF and cohesin, and repeat DNA sequences affecting
130 the expression level of genes, EPI were predicted based on EPA shortened at the
131 genomic locations of the DNA motif sequence of a TF or a repeat DNA sequence, and
132 transcriptional target genes of each TF bound in enhancers and promoters were
133 predicted based on the EPI. The expression levels of the putative transcriptional target
134 genes were compared with those predicted from promoters using Mann Whiteney U test
135 (p-value < 0.05) (Fig. 2). The number of TF showing a significant difference of
136 expression level of their putative transcriptional target genes was counted. To examine
137 whether the orientation of a DNA motif sequence, which is supposed to act as insulator
138 sites and shorten EPA, affected the number of TF showing a significant difference of
139 expression level of their putative transcriptional target genes, the number of the TF was
140 compared among forward-reverse (FR), reverse-forward (RF), and any orientation (i.e.
141 without considering orientation) of a DNA motif sequence shortening EPA, using
142 chi-square test (p-value < 0.05). To avoid missing DNA motif sequences showing a

143 relatively weak statistical significance by multiple testing collection, the above analyses
144 were conducted using monocytes of four people independently, and DNA motif
145 sequences found in monocytes of four people in common were selected. Total 287 of
146 biased (159 FR and 153 RF) orientation of DNA binding motif sequences of TF were
147 found in monocytes of four people in common, whereas only one any orientation of
148 DNA binding motif sequence was found in monocytes of four people in common (Fig.
149 3; Table 1; Supplemental Table S1). FR orientation of DNA motif sequences included
150 CTCF, cohesin (RAD21 and SMC3), ZNF143 and YY1, which are associated with
151 chromatin interactions and EPI. SMARCA4 (BRG1) is associated with topologically
152 associated domain (TAD), which is higher-order chromatin organization. The DNA
153 binding motif sequences of SMARCA4 was not registered in the databases used in this
154 study. FR orientation of DNA motif sequences included SMARCC2, a member of the
155 same SWI/SNF family of proteins as SMARCA4.

156 The same analysis was conducted using DNase-seq data of $CD4^+$ T cells of four
157 people. Total 265 of biased (158 FR and 139 RF) orientation of DNA binding motif
158 sequences of TF were found in T cells of four people in common, whereas only four any
159 orientation (i.e. without considering orientation) of DNA binding motif sequences were
160 found in T cells of four people in common (Supplemental Fig. S1 and Supplemental
161 Table S2). Biased orientation of DNA motif sequences in T cells included CTCF,
162 cohesin (RAD21 and SMC3), ZNF143, YY1, and SMARC. Biased orientation of DNA
163 motif sequences in T cells and monocytes (using H3K27ac histone modification marks,
164 which is described in the next paragraph) included JUNDM2 (JDP2), which is involved

165 in histone-chaperone activity, promoting nucleosome, and inhibition of histone
166 acetylation (Jin et al. 2006). JDP2 forms a homodimer or heterodimer with various TF
167 (https://en.wikipedia.org/wiki/Jun_dimerization_protein). Among 287, 61 of biased
168 orientation of DNA binding motif sequences of TF were found in both monocytes and T
169 cells in common (Supplemental Table S5). For each orientation, 31 FR and 34 RF
170 orientation of DNA binding motif sequences of TF were found in both monocytes and T
171 cells in common. Without considering the difference of orientation of DNA binding
172 motif sequences, 84 of biased orientation of DNA binding motif sequences of TF were
173 found in both monocytes and T cells. As a reason for the increase of the number (84)
174 from 61, a TF or an isoform of the same TF may bind to a different DNA binding motif
175 sequence according to cell types and/or in the same cell type. About 50% or more of
176 alternative splicing isoforms are differently expressed among tissues, indicating that
177 most alternative splicing is subject to tissue-specific regulation (Wang et al. 2008)
178 (Chen and Manley 2009) (Das et al. 2007). The same TF has several DNA binding
179 motif sequences and in some cases one of the motif sequences is almost the same as the
180 reverse complement sequence of another motif sequence of the same TF. For example,
181 RAD21 had both FR and RF orientation of DNA motif sequences, but the number of the
182 FR orientation of DNA motif sequence was relatively small in the genome, and the RF
183 orientation of DNA motif sequence was frequently observed and co-localized with
184 CTCF. I previously found that a complex of TF would bind to a slightly different DNA
185 binding motif sequence from the combination of DNA binding motif sequences of TF
186 composing the complex in *C. elegans* (Tabuchi et al. 2011). From another viewpoint of

187 this study, the expression level of putative transcription target genes of some TF would
188 be different, depending on the genomic locations (enhancers or promoters) of DNA
189 binding motif sequences of the TF in monocytes and T cells of four people.

190 Moreover, using open chromatin regions overlapped with H3K27ac histone
191 modification marks known as enhancer and promoter marks, the same analyses were
192 performed in monocytes and T cells. H3K27ac histone modification marks were used in
193 the analysis of EPI, but were not used in the analysis of TF as insulator like CTCF and
194 cohesin in this study, since new biased orientation of DNA motif sequences were found
195 in this criterion. When H3K27ac histone modification marks were used in the analysis
196 of TF as insulator like CTCF and cohesin, the number of biased orientation of DNA
197 motif sequences was decreased. Total 241 of biased (141 FR and 120 RF) orientation of
198 DNA binding motif sequences of TF were found in monocytes of four people in
199 common, whereas only one any orientation of DNA binding motif sequence was found
200 (Supplemental Table S3). Though the number of biased orientation of DNA motif
201 sequences was reduced, JDP2 was found in monocytes as well as T cells. CTCF,
202 RAD21, SMC3, ZNF143, YY1, and SMARCC2 were also found. For T cells using
203 H3K27ac histone modification marks, total 195 of biased (107 FR and 110 RF)
204 orientation of DNA binding motif sequences of TF were found in T cells of four people
205 in common, whereas only six any orientation of DNA binding motif sequences were
206 found (Supplemental Table S4). Though the number of biased orientation of DNA motif
207 sequences was reduced, CTCF, RAD21, SMC3, YY1, and SMARCC2 were found.
208 Scores of CTCF, RAD21, and SMC3 were increased compared with the result of T cells

209 without using H3K27ac histone modification marks, and they were ranked in the top six.
210 As summary of the results with and without H3K27ac histone modification marks, total
211 386 of biased (223 FR and 214 RF) orientation of DNA motif sequences were found in
212 monocytes of four people in common. Total 348 of biased (202 FR and 198 RF)
213 orientation of DNA motif sequences were found in T cells of four people in common.
214 Total number of these results in monocytes and T cells was 590 biased (368 FR and 359
215 RF) orientation of DNA motif sequences. Biased orientation of DNA motif sequences
216 found in both monocytes and T cells were listed in Supplemental Table S5.

217 To examine whether the biased orientation of DNA binding motif sequences of
218 TF were observed in other cell types, the same analyses were conducted in other cell
219 types. However, for other cell types, experimental data of one sample were available in
220 ENCODE database, so the analyses of DNA motif sequences were performed by
221 comparing with the result in monocytes of four people. Among the biased orientation of
222 DNA binding motif sequences found in monocytes, 69, 82, 56, and 53 DNA binding
223 motif sequences were also observed in H1-hESC, iPS, Huvec and MCF-7 respectively,
224 including CTCF and cohesin (RAD21 and SMC3) (Table 2; Supplemental Table S6).
225 The scores of DNA binding motif sequences were the highest in monocytes, and the
226 other cell types showed lower scores. The results of the analysis of DNA motif
227 sequences in $CD20^{+}$ B cells and macrophages did not include CTCF and cohesin,
228 because these analyses can be utilized in cells where the expression level of putative
229 transcriptional target genes of each TF show a significant difference between promoters
230 and EPA shortened at the genomic locations of a DNA motif sequence acting as

231 insulator sites. Some experimental data of a cell did not show a significant difference
232 between promoters and the EPA (Osato 2018).

233 Instead of DNA binding motif sequences of TF, repeat DNA sequences were also
234 examined. The expression levels of transcriptional target genes of each TF predicted
235 based on EPA that were shortened at the genomic locations of a repeat DNA sequence
236 were compared with those predicted from promoters. Three RF orientation of repeat
237 DNA sequences showed a significant difference of expression level of putative
238 transcriptional target genes in monocytes of four people in common (Table 3). Among
239 them, LTR16C repeat DNA sequence was observed in iPS and H1-hESC with enough
240 statistical significance considering multiple tests (p-value $< 10^{-7}$). The same as $CD14^+$
241 monocytes, biased orientation of repeat DNA sequences were examined in $CD4^+$ T cells.
242 Three FR and two RF orientation of repeat DNA sequences showed a significant
243 difference of expression level of putative transcriptional target genes in T cells of four
244 people in common (Supplemental Table S7). MIRb and MIR3 were also found in the
245 analysis using open chromatin regions overlapped with H3K27ac histone modification
246 marks, which are enhancer and promoter marks. MIR and other transposon sequences
247 are known to act as insulators and enhancers (Bejerano et al. 2006; Rebollo et al. 2012;
248 de Souza et al. 2013; Jjingo et al. 2014; Wang et al. 2015).

249

250 **Co-location of biased orientation of DNA motif sequences**

251 To examine the association of 287 biased (FR and RF) orientation of DNA
252 binding motif sequences of TF, co-location of the DNA binding motif sequences in open

253 chromatin regions was analyzed in monocytes. The number of open chromatin regions
254 with the same pairs of DNA binding motif sequences was counted, and when the pairs
255 of DNA binding motif sequences were enriched with statistical significance (chi-square
256 test, p-value $< 1.0 \times 10^{-10}$), they were listed (Table 4; Supplemental Table S8). Open
257 chromatin regions overlapped with histone modification of enhancer and promoter
258 marks (H3K27ac) (total 26,095 regions) showed a larger number of enriched pairs of
259 DNA motifs than all open chromatin regions (Table 4; Supplemental Table S8).
260 H3K27ac is known to be enriched at chromatin interaction anchors (Phanstiel et al.
261 2017). As already known, CTCF was found with cohesin such as RAD21 and SMC3
262 (Table 4). Top 30 pairs of FR and RF orientations of DNA motifs co-occupied in the
263 same open chromatin regions were shown (Table 4). Total number of pairs of DNA
264 motifs was 492, consisting of 115 unique DNA motifs, when the pair of DNA motifs
265 were observed in more than 80% of the number of open chromatin regions with the
266 DNA motifs. Biased orientation of DNA binding motif sequences of TF tended to be
267 co-localized in the same open chromatin regions.

268 To examine the association of 265 biased orientation of DNA binding motif
269 sequences of TF in $CD4^+$ T cells, co-location of the DNA binding motif sequences in
270 open chromatin regions was analyzed. Top 30 pairs of FR and RF orientations of DNA
271 motifs co-occupied in the same open chromatin regions were shown (Supplemental
272 Table S9). Total number of pairs of DNA motifs was 332, consisting of 118 unique
273 DNA motifs, when the pair of DNA motifs were observed in more than 60% of the
274 number of open chromatin regions with the DNA motifs (chi-square test, p-value < 1.0

275 $\times 10^{-10}$). Among them, 12 pairs of DNA motif sequences including a pair of CTCF,
276 SMC3, and RAD21 in T cells were found in monocytes in common (Supplemental
277 Table S9).
278
279 **Pairs of biased orientation of DNA motif sequences surrounding genes**
280 CTCF and cohesin are found in chromatin interaction anchors and are considered
281 to form homodimers. TF are also known to form heterodimers with another TF. In this
282 study, if the DNA binding motif sequence of only the mate to a pair of TF was found in
283 EPA, EPA was shortened at one side, which is the genomic location of the DNA binding
284 motif sequence of the mate to the pair, and transcriptional target genes were predicted
285 using the EPA shortened at the side. In this analysis, the mate to both heterodimer and
286 homodimer of TF can be used to examine the effect on the expression level of
287 transcriptional target genes predicted based on the EPA shortened at one side. To
288 examine whether biased orientation of DNA motif sequences tend to be found as a pair
289 of the same TF or different TF in upstream and downstream of genes, the enrichment of
290 pairs of biased orientation of DNA motif sequences was investigated. The number of
291 genes with a pair of FR or RF orientation of DNA motif sequences was counted using
292 all pairs of the DNA motif sequences, and statistical tests (chi-square test) were
293 conducted. The total number of genes (transcripts) with a biased orientation of DNA
294 motif sequence in their upstream or/and downstream was about 20,000. This is almost
295 the same way of analysis as co-location of biased orientation of DNA motif sequences,
296 and the analysis here used the number of genes instead of open chromatin regions. Fig.

297 4 and Supplemental Fig. S2 showed that not only pairs of the same TF, but also pairs of
298 different TF were found in upstream and downstream of genes. The number of DNA
299 motif sequences of the same TF was assigned independently in each figure of heat map,
300 so for example, 'CTCF_1' in Fig. 4 may not be the same DNA motif sequence of
301 'CTCF_1' in another figure in Supplemental Fig. S2. DNA motif sequences of CTCF
302 and cohesin (RAD21 and SMC3) were enriched near the same genes, but cohesin
303 tended to be found with another TF near the same genes as well. The number of some
304 pairs of biased orientation of DNA motif sequences in genome sequences was small,
305 though they showed statistical significance (Supplemental material 2). The result of the
306 analysis seems to be different between monocytes and T cells and between using
307 H3K27ac histone modification marks and not using them (Supplemental Fig. S2). Some
308 of these TF would form homodimers or heterodimers directory or indirectly composing
309 a complex structure, contributing to make chromatin interactions (Fig. 6).
310

311 **Comparison with chromatin interaction data**

312 To examine whether the biased orientation of DNA motif sequences is associated
313 with chromatin interactions, enhancer-promoter interactions (EPI) predicted based on
314 enhancer-promoter associations (EPA) were compared with chromatin interaction data
315 (Hi-C). Due to the resolution of Hi-C experimental data used in this study (50kb), EPI
316 were adjusted to 50kb resolution. EPI were predicted based on three types of EPA: (i)
317 EPA without being shortened by the genomic locations of a DNA motif sequence, (ii)
318 EPA shortened at the genomic locations of the DNA motif sequence of TF acting as

319 insulator sites such as CTCF and cohesin (RAD21, SMC3) without considering their
320 orientation, and (iii) EPA shortened at the genomic locations of FR or RF orientation of
321 DNA motif sequence of TF. EPA (iii) showed significantly a higher ratio of EPI
322 overlapped with chromatin interactions (Hi-C) using DNA binding motif sequences of
323 CTCF and cohesin (RAD21 and SMC3) than the other two types of EPAs
324 (Supplemental Fig. S3). Total 59 biased orientation (40 FR and 23 RF) of DNA motif
325 sequences including CTCF, cohesin, and YY1 showed significantly a higher ratio of EPI
326 overlapped with Hi-C chromatin interactions (a cutoff score of CHiCAGO tool > 1)
327 than the other types of EPAs in monocytes (Supplemental Table S10). When comparing
328 EPI predicted based on only (i) and (iii) with chromatin interactions, total 174 biased
329 orientation (101 FR and 84 RF) of DNA motif sequences showed significantly a higher
330 ratio of EPI predicted based on (iii) overlapped with the chromatin interactions than EPI
331 predicted based on (i) (Supplemental material 2). The difference between EPI predicted
332 based on (ii) and (iii) seemed to be difficult to distinguish using the chromatin
333 interaction data and the statistical test in some cases. However, as for the difference
334 between EPI predicted based on (i) and (iii), a larger number of biased orientation of
335 DNA motif sequences was found to be correlated with chromatin interaction data.
336 Chromatin interaction data were obtained from different samples from DNase-seq, open
337 chromatin regions, so individual differences seemed to be large from the results of this
338 analysis. Since, for some DNA motif sequences of transcription factors, the number of
339 EPI overlapped with chromatin interactions was small, if higher resolution of chromatin
340 interaction data (such as HiChIP, in situ DNase Hi-C, and in situ Hi-C data, or a tool to

341 improve the resolution such as HiCPlus) is available, the number of EPI overlapped
342 with chromatin interactions would be increased and the difference of the numbers
343 among three types of EPA might be larger and more significant (Rao et al. 2014;
344 Ramani et al. 2016; Mumbach et al. 2017; Zhang et al. 2018).

345 After the analysis of $CD14^+$ monocytes, to utilize HiChIP chromatin interaction
346 data in $CD4^+$ T cells, the same analysis for $CD14^+$ monocytes was performed using
347 DNase-seq data of four donors in $CD4^+$ T cells (Mumbach et al. 2017). EPI predicted
348 based on EPA were compared with HiChIP chromatin interaction data in $CD4^+$ T cells.
349 The resolutions of HiChIP chromatin interaction data and EPI were adjusted to 5kb. EPI
350 were predicted based on the three types of EPA in the same way as $CD14^+$ monocytes
351 using top 60% of all the transcript (gene) excluding transcripts not expressed in T cells.
352 The criteria of the analysis were determined to include known DNA motif sequences
353 involved in chromatin interactions such as CTCF and cohesin in the result, and the
354 result was consistent with the result using Hi-C chromatin interaction data. EPA (iii)
355 showed the highest ratio of EPI overlapped with chromatin interactions (HiChIP) using
356 DNA binding motif sequences of CTCF and cohesin (RAD21 and SMC3), compared
357 with the other two types of EPAs (Fig. 5). Total 121 biased orientation (73 FR and 58
358 RF) of DNA motif sequences including CTCF, cohesin, ZNF143, and SMARC showed
359 a higher ratio of EPI overlapped with HiChIP chromatin interactions (more than 1,000
360 counts for each interaction) than the other types of EPAs in T cells (Table 5). When
361 comparing EPI predicted based on only (i) and (iii) with the chromatin interactions,
362 total 226 biased orientation (132 FR and 123 RF) of DNA motif sequences showed a

363 higher ratio of EPI predicted based on (iii) overlapped with the chromatin interactions
364 than EPI predicted based on (i) (Supplemental material 2). As expected, the number of
365 EPI overlapped with chromatin interactions (HiChIP) was increased, compared with
366 Hi-C chromatin interactions. Most of biased orientation of DNA motif sequences (85%)
367 were found to be correlated with chromatin interactions, when comparing EPI predicted
368 based on (i) and (iii) with HiChIP chromatin interactions.

369 Though the ratios of EPI overlapped with chromatin interactions were increased
370 by using many chromatin interaction data including lower score and count of chromatin
371 interactions (a cutoff score of CHiCAGO tool > 1 for Hi-C and more than 1,000 counts
372 for HiChIP), the ratios of EPI overlapped with chromatin interactions showed the same
373 tendency among three types of EPA (FR, any and others). The ratio of EPI overlapped
374 with Hi-C chromatin interactions was increased using H3K27ac marks in both
375 monocytes and T cells. The ratio of EPI overlapped with HiChIP chromatin interactions
376 was also increased using H3K27ac marks. The same as $CD14^+$ monocytes, chromatin
377 interaction data were obtained from different samples from DNase-seq, open chromatin
378 regions in $CD4^+$ T cells, so individual differences seemed to be large from the results of
379 this analysis, and (Mumbach et al. 2017) suggested that individual differences of
380 chromatin interactions were larger than those of open chromatin regions. ATAC-seq data,
381 open chromatin regions were available in $CD4^+$ T cells in the paper, however, when
382 using ATAC-seq data, the result of the analysis of biased orientation of DNA motif
383 sequences was different from DNase-seq data, and not included a part of CTCF and
384 cohesin. Thus, DNase-seq data collected from ENCODE and Blueprint projects were

385 employed in this study.

386

387 **Discussion**

388 To find DNA motif sequences of transcription factors (TF) and repeat DNA
389 sequences affecting the expression level of human putative transcriptional target genes,
390 the DNA motif sequences were searched from open chromatin regions of monocytes of
391 four people. Total 287 biased [159 forward-reverse (FR) and 153 reverse-forward (RF)]
392 orientation of DNA motif sequences of TF were found in monocytes of four people in
393 common, whereas only one any orientation (i.e. without considering orientation) of
394 DNA motif sequence of TF was found to affect the expression level of putative
395 transcriptional target genes, suggesting that enhancer-promoter association (EPA)
396 shortened at the genomic locations of FR or RF orientation of the DNA motif sequence
397 of a TF or a repeat DNA sequence is an important character for the prediction of
398 enhancer-promoter interactions (EPI) and the transcriptional regulation of genes.

399 When DNA motif sequences were searched from monocytes of one person, a
400 larger number of biased orientation of DNA motif sequences affecting the expression
401 level of human putative transcriptional target genes were found. When the number of
402 donors, from which experimental data were obtained, was increased, the number of
403 DNA motif sequences found in all people in common decreased and in some cases,
404 known transcription factors involved in chromatin interactions such as CTCF and
405 cohesin (RAD21 and SMC3) were not identified by statistical tests. This would be
406 caused by individual difference of the same cell type, low quality of experimental data,

407 and experimental errors. Moreover, though FR orientation of DNA binding motif
408 sequences of CTCF and cohesin is frequently observed at chromatin interaction anchors,
409 the percentage of FR orientation is not 100, and other orientations of the DNA binding
410 motif sequences are also observed. Though DNA binding motif sequences of CTCF and
411 cohesin are found in various open chromatin regions, DNA binding motif sequences of
412 some TF would be observed less frequently in open chromatin regions. The analyses of
413 experimental data of a number of people would avoid missing relatively weak statistical
414 significance of DNA motif sequences of TF in experimental data of each person by
415 multiple testing correction of thousands of statistical tests. A DNA motif sequence was
416 found with p-value < 0.05 in experimental data of one person and the DNA motif
417 sequence found in the same cell type of four people in common would have p-value $<$
418 $0.05^4 = 0.00000625$. Actually, DNA motif sequences with p-value slightly less than 0.05
419 in monocytes of one person were observed in monocytes of four people in common.

420 EPI were compared with chromatin interactions (Hi-C) in monocytes. EPAs
421 shortened at the genomic locations of DNA binding motif sequences of CTCF and
422 cohesin (RAD21 and SMC3) showed a significant difference of the ratios of EPI
423 overlapped with chromatin interactions, according to three types of EPAs (see Methods).
424 Using open chromatin regions overlapped with ChIP-seq experimental data of histone
425 modification of an enhancer mark (H3K27ac), the ratio of EPI not overlapped with
426 Hi-C was reduced. (Phanstiel et al. 2017) also reported that there was an especially
427 strong enrichment for loops with H3K27 acetylation peaks at both ends (Fisher's Exact
428 Test, $p = 1.4 \times 10^{-27}$). However, the total number of EPI overlapped with chromatin

429 interactions was also reduced using H3K27ac peaks, so more chromatin interaction data
430 would be needed to obtain reliable results in this analysis. As an issue of experimental
431 data, data for chromatin interactions and open chromatin regions were came from
432 different samples and donors, so individual differences would exist in the data.
433 Moreover, the resolution of chromatin interaction data used in monocytes is about 50kb,
434 thus the number of chromatin interactions was relatively small (72,284 at 50kb
435 resolution with a cutoff score of CHiCAGO tool > 1 and 16,501 with a cutoff score of
436 CHiCAGO tool > 5). EPI predicted based on EPA shortened at the genomic locations of
437 DNA binding motif sequence of TF that were found in various open chromatin regions
438 such as CTCF and cohesin (RAD21 and SMC3) tend to be overlapped with a larger
439 number of chromatin interactions than TF less frequently observed in open chromatin
440 regions. Therefore, to examine the difference of the numbers of EPI overlapped with
441 chromatin interactions, according to three types of EPAs, the number of chromatin
442 interactions should be large enough.

443 As HiChIP chromatin interaction data were available in $CD4^+$ T cells, biased
444 orientation of DNA motif sequences of TF were examined in T cells using DNase-seq
445 data of four people. The resolutions of chromatin interactions and EPI were adjusted to
446 5kb by fragmentation of genome sequences. In monocytes, the resolution of Hi-C
447 chromatin interaction data was converted by extending anchor regions of chromatin
448 interactions to 50kb length and merging the chromatin interactions overlapped with
449 each other. Fragmentation of genome sequences may affect the classification of
450 chromatin interactions of which anchors are located near the border of a fragment, but

451 the number of chromatin interactions would not be decreased, compared with merging
452 chromatin interactions. The number of HiChIP chromatin interactions was 19,926,360
453 at 5kb resolution, 666,149 at 5kb resolution with chromatin interactions (more than
454 1,000 counts for each interaction), and 78,209 at 5kb resolution with chromatin
455 interactions (more than 6,000 counts for each interaction). As expected, the number of
456 EPI overlapped with chromatin interactions was increased, and 46 – 85% of biased
457 orientation of DNA motif sequences of TF showed a statistical significance in EPI
458 predicted based on EPA shortened at the genomic locations of the DNA motif sequence,
459 compared with the other types of EPAs or EPA not shortened. False positive predictions
460 of EPI would be decreased by using H3K27ac marks and other features. The ratio of
461 EPI overlapped with Hi-C chromatin interactions was increased using H3K27ac marks
462 in both monocytes and T cells. The ratio of EPI overlapped with HiChIP chromatin
463 interactions was also increased using H3K27ac marks. However, the number of biased
464 orientation of DNA motif sequences showing a higher ratio of EPI overlapped with
465 HiChIP chromatin interactions than the other types of EPAs was decreased using
466 H3K27ac marks (Supplemental material 2).

467 Though the number of known DNA binding proteins and TF involved in
468 chromatin interactions would be less than 30 or so, about 300 DNA binding proteins
469 showed enrichment of biased orientation of their DNA binding sequences, and known
470 DNA binding proteins involved in chromatin interactions were found in the biased
471 orientation of DNA binding sequences. JUNDM2 (JDP2) found in T cells and
472 monocytes is not known DNA binding proteins involved in chromatin interactions.

473 JDP2 is involved in histone and nucleosome-related functions such as
474 histone-chaperone activity, promoting nucleosome, and inhibition of histone acetylation
475 (Jin et al. 2006). JDP2 forms a homodimer or heterodimer with various TF
476 (https://en.wikipedia.org/wiki/Jun_dimerization_protein). Thus, the main function of
477 JDP2 may not be associated with chromatin interactions, but it forms a homodimer or
478 heterodimer with TF, potentially forming a chromatin interaction through the binding of
479 JDP2 and another TF, like chromatin interactions formed by YY1 (Weintraub et al.
480 2017). In the analysis of HiChIP chromatin interaction data, JDP2 was in the list of
481 biased orientation of DNA motif sequences showing a higher ratio of EPI overlapped
482 with HiChIP chromatin interactions than the other types of EPAs, using chromatin
483 interactions with more than 6,000 counts (Supplemental material 2). When forming a
484 homodimer or heterodimer with another TF, TF may bind to genome DNA with a
485 specific orientation of their DNA binding sequences. From the analysis of biased
486 orientation of DNA motif sequences of TF, TF forming heterodimer would also be
487 found. If the DNA binding motif sequence of only the mate to a pair of TF was found in
488 EPA, EPA was shortened at one side, which is the genomic location of the DNA binding
489 motif sequence of the mate to the pair, and transcriptional target genes were predicted
490 using the EPA shortened at the side. In this analysis, the mate to both heterodimer and
491 homodimer of TF can be used to examine the effect on the expression level of
492 transcriptional target genes predicted based on the EPA shortened at one side. For
493 heterodimer, biased orientation of DNA motif sequences may also be found in
494 forward-forward or reverse-reverse orientation.

495 I reported that the ratio of the number of functional enrichment of putative
496 transcriptional target genes in the total number of putative transcriptional target genes
497 changed according to the types of EPA, in the same way as gene expression level (Osato
498 2018). JDP2 showed a higher ratio of functional enrichment of putative transcriptional
499 target genes using EPA shortened at the genomic locations of FR orientation of the DNA
500 binding motif sequence, compared with the other types of EPAs (RF or any orientation)
501 in monocytes and T cells, among monocytes, T cells and $CD20^{+}$ B cells. While the
502 genome-wide analysis of functional enrichment of putative transcriptional target genes
503 takes computational time, the genome-wide analysis of gene expression level is finished
504 with less computational time. The analysis of gene expression level can be used for a
505 cell type and experimental data where the expression levels of transcriptional target
506 genes predicted based on EPA are significantly different from those predicted from only
507 promoter.

508 It has been reported that CTCF and cohesin-binding sites are frequently mutated
509 in cancer (Katainen et al. 2015). Some biased orientation of DNA motif sequences
510 would be associated with chromatin interactions and might be associated with diseases
511 including cancer.

512 The analyses in this study revealed novel characters of DNA binding motif
513 sequences of TF and repeat DNA sequences, and would be useful to analyze TF
514 involved in chromatin interactions and/or forming a homodimer, heterodimer or
515 complex with other TF, affecting the transcriptional regulation of genes.

516

517 # Methods

518 **Search for biased orientation of DNA motif sequences**

519 To examine transcriptional regulatory target genes of transcription factors (TF),
520 bed files of hg38 of Blueprint DNase-seq data for $CD14^+$ monocytes of four donors
521 (EGAD00001002286; Donor ID: C0010K, C0011I, C001UY, C005PS) were obtained
522 from Blueprint project web site (http://dcc.blueprint-epigenome.eu/#/home), and the bed
523 files of hg38 were converted into those of hg19 using Batch Coordinate Conversion
524 (liftOver) web site (https://genome.ucsc.edu/util.html). Bed files of hg19 of ENCODE
525 H1-hESC (GSM816632; UCSC Accession: wgEncodeEH000556), iPSC (GSM816642;
526 UCSC Accession: wgEncodeEH001110), HUVEC (GSM1014528; UCSC Accession:
527 wgEncodeEH002460), and MCF-7 (GSM816627; UCSC Accession:
528 wgEncodeEH000579) were obtained from the ENCODE websites
529 (http://hgdownload.cse.ucsc.edu/goldenPath/hg19/encodeDCC/wgEncodeUwDgf/;
530 http://hgdownload.cse.ucsc.edu/goldenPath/hg19/encodeDCC/wgEncodeUwDnase/).

531 As high resolution of chromatin interaction data using HiChIP became available
532 in $CD4^+$ T cells, to promote the same analysis of $CD14^+$ monocytes in $CD4^+$ T cells,
533 DNase-seq data of four donors were obtained from a public database and Blueprint
534 projects web sites. DNase-seq data of only one donor was available in Blueprint project
535 for $CD4^+$ T cells (Donor ID: S008H1), and three other DNase-seq data were obtained
536 from NCBI Gene Expression Omnibus (GEO) database. Though the peak calling of
537 DNase-seq data available in GEO database was different from other DNase-seq data in
538 ENCODE and Blueprint projects where 150bp length of peaks were usually predicted

539 using HotSpot (John et al. 2011), FASTQ files of DNase-seq data were downloaded
540 from NCBI Sequence Read Archive (SRA) database (SRR097566, SRR097618, and
541 SRR171574). Read sequences of the FASTQ files were aligned to the hg19 version of
542 the human genome reference using BWA (Li and Durbin 2009), and the BAM files
543 generated by BWA were converted into SAM files, sorted, and indexed using Samtools
544 (Li et al. 2009). Peaks of the DNase-seq data were predicted using HotSpot-4.1.1.

545 To identify transcription factor binding sites (TFBS) from the DNase-seq data,
546 TRANSFAC (2013.2), JASPAR (2010), UniPROBE, BEEML-PBM, high-throughput
547 SELEX, Human Protein-DNA Interactome, and transcription factor binding sequences
548 of ENCODE ChIP-seq data were used (Wingender et al. 1996; Newburger and Bulyk
549 2009; Portales-Casamar et al. 2010; Xie et al. 2010; Zhao and Stormo 2011; Jolma et al.
550 2013; Kheradpour and Kellis 2014). Position weight matrices of transcription factor
551 binding sequences were transformed into TRANSFAC matrices and then into MEME
552 matrices using in-house scripts and transfac2meme in MEME suite (Bailey et al. 2009).
553 Transcription factor binding sequences of TF derived from vertebrates were used for
554 further analyses. Transcription factor binding sequences were searched from each
555 narrow peak of DNase-seq data using FIMO with *p*-value threshold of 10^{-5} (Grant et al.
556 2011). TF corresponding to transcription factor binding sequences were searched
557 computationally by comparing their names and gene symbols of HGNC (HUGO Gene
558 Nomenclature Committee) -approved gene nomenclature and 31,848 UCSC known
559 canonical transcripts
560 (http://hgdownload.cse.ucsc.edu/goldenpath/hg19/database/knownCanonical.txt.gz), as

561 transcription factor binding sequences were not linked to transcript IDs such as UCSC,
562 RefSeq, and Ensembl transcripts.

563 Target genes of a TF were assigned when its TFBS was found in DNase-seq
564 narrow peaks in promoter or extended regions for enhancer-promoter association of
565 genes (EPA). Promoter and extended regions were defined as follows: promoter regions
566 were those that were within distance of ±5 kb from transcriptional start sites (TSS).
567 Promoter and extended regions were defined as per the following association rule,
568 which is the same as that defined in Figure 3A of a previous study (McLean et al. 2010):
569 the single nearest gene association rule, which extends the regulatory domain to the
570 midpoint between the TSS of the gene and that of the nearest gene upstream and
571 downstream without the limitation of extension length. Extended regions for EPA were
572 shortened at the genomic locations of DNA binding sites of TF that were the closest to a
573 transcriptional start site, and transcriptional target genes were predicted from the
574 shortened enhancer regions using TFBS. Furthermore, promoter and extended regions
575 for EPA were shortened at the genomic locations of forward–reverse (FR) orientation of
576 DNA binding sites of TF. When forward or reverse orientation of DNA binding sites
577 were continuously located in genome sequences several times, the most external
578 forward–reverse orientation of DNA binding sites were selected. The genomic positions
579 of genes were identified using 'knownGene.txt.gz' file in UCSC bioinformatics sites
580 (Karolchik et al. 2014). The file 'knownCanonical.txt.gz' was also utilized for choosing
581 representative transcripts among various alternate forms for assigning promoter and
582 extended regions for EPA. From the list of transcription factor binding sequences and

583 transcriptional target genes, redundant transcription factor binding sequences were
584 removed by comparing the target genes of a transcription factor binding sequence and
585 its corresponding TF; if identical, one of the transcription factor binding sequences was
586 used. When the number of transcriptional target genes predicted from a transcription
587 factor binding sequence was less than five, the transcription factor binding sequence
588 was omitted.

589 Repeat DNA sequences were searched from the hg19 version of the human
590 reference genome using RepeatMasker (Smit, AFA & Green, P RepeatMasker at
591 http://www.repeatmasker.org) and RepBase RepeatMasker Edition
592 (http://www.girinst.org).

593 For gene expression data, RNA-seq reads mapped onto human hg19 genome
594 sequences were obtained, including ENCODE long RNA-seq reads with poly-A of
595 H1-hESC, iPSC, HUVEC, and MCF-7 (GSM26284, GSM958733, GSM2344099,
596 GSM2344100, GSM958734, and GSM765388), and UCSF-UBC human reference
597 epigenome mapping project RNA-seq reads with poly-A of naive $CD4^+$ T cells
598 (GSM669617). Two replicates were present for H1-hESC, iPSC, HUVEC, and MCF-7,
599 and a single one for $CD4^+$ T cells. RPKMs of the RNA-seq data were calculated using
600 RSeQC (Wang et al. 2012). For monocytes, Blueprint RNA-seq RPKM data
601 (GSE58310, GSE58310_GeneExpression.csv.gz, Monocytes_Day0_RPMI) were used
602 (Saeed et al. 2014). Based on RPKM, UCSC transcripts with expression level among
603 top 30% of all the transcripts were selected in each cell type.

604 The expression level of transcriptional target genes predicted based on EPA

605 shortened at the genomic locations of DNA motif sequence of a TF or a repeat DNA
606 sequence was compared with the expression level of transcriptional target genes
607 predicted from promoter. For each DNA motif sequence shortening EPA, transcriptional
608 target genes were predicted using about 3,000 – 5,000 DNA binding motif sequences of
609 TF, and the expression level of putative transcriptional target genes of each TF was
610 compared between EPA and only promoter using Mann-Whitney test (p-value < 0.05).
611 The number of TF showing a significant difference of expression level of putative
612 transcriptional target genes between EPA and promoter was compared among
613 forward-reverse (FR), reverse-forward (RF), and any orientation (i.e. without
614 considering orientation) of a DNA motif sequence shortening EPA using chi-square test
615 (p-value < 0.05). When a DNA motif sequence of a TF or a repeat DNA sequence
616 shortening EPA showed a significant difference of expression level of putative
617 transcriptional target genes among FR, RF, or any orientation in monocytes of four
618 people in common, the DNA motif sequences were listed.

619 Though forward-reverse orientation of DNA binding motif sequences of CTCF
620 and cohesin is frequently observed at chromatin interaction anchors, the percentage of
621 forward-reverse orientation is not 100, and other orientations of the DNA binding motif
622 sequences are also observed. Though DNA binding motif sequences of CTCF and
623 cohesin are found in various open chromatin regions, DNA binding motif sequences of
624 some transcription factors would be observed less frequently in open chromatin regions.
625 The analyses of experimental data of a number of people would avoid missing relatively
626 weak statistical significance of DNA motif sequences in experimental data of each

627 person by multiple testing correction of thousands of statistical tests. A DNA motif
628 sequence was found with p-value < 0.05 in experimental data of one person and the
629 DNA motif sequence found in the same cell type of four people in common would have
630 p-value < 0.05^4 = 0.00000625.
631
632 **Co-location of biased orientation of DNA motif sequences**
633 Co-location of biased orientation of DNA binding motif sequences of TF was
634 examined. The number of open chromatin regions with the same pair of DNA binding
635 motif sequences was counted, and when the pair of DNA binding motif sequences were
636 enriched with statistical significance (chi-square test, p-value < 1.0×10^{-10}), they were
637 listed.
638 For histone modification of an enhancer mark (H3K27ac), bed files of hg38 of
639 Blueprint ChIP-seq data for $CD14^+$ monocytes (EGAD00001001179) and $CD4^+$ T cells
640 (Donor ID: S000RD) were obtained from Blueprint web site
641 (http://dcc.blueprint-epigenome.eu/#/home), and the bed files of hg38 were converted
642 into those of hg19 using Batch Coordinate Conversion (liftOver) web site
643 (https://genome.ucsc.edu/util.html).
644
645 **Comparison with chromatin interaction data**
646 For comparison of EPA in monocytes with chromatin interactions,
647 'PCHiC_peak_matrix_cutoff0.txt.gz' file was downloaded from 'Promoter Capture
648 Hi-C in 17 human primary blood cell types' web site (https://osf.io/u8tzp/files/), and

649 chromatin interactions for Monocytes with scores of CHiCAGO tool > 1 and
650 CHiCAGO tool > 5 were extracted from the file (Javierre et al. 2016). In the same way
651 as monocytes, Hi-C chromatin interaction data of $CD4^+$ T cells (Naive $CD4^+$ T cells,
652 nCD4) were obtained.

653 Enhancer-promoter interactions (EPI) were predicted using three types of EPAs in
654 monocytes: (i) EPA shortened at the genomic locations of FR or RF orientation of DNA
655 motif sequence of TF, (ii) EPA shortened at the genomic locations of any orientation (i.e.
656 without considering orientation) of DNA motif sequence of TF, and (iii) EPA without
657 being shortened by a DNA motif sequence. EPI predicted using the three types of EPAs
658 in common were removed. First, EPI predicted based on EPA (i) were compared with
659 chromatin interactions (Hi-C). The resolution of chromatin interaction data used in this
660 study was 50kb, so EPI were adjusted to 50kb before their comparison. The number and
661 ratio of EPI overlapped with chromatin interactions were counted. Second, EPI were
662 predicted based on EPA (ii), and EPI predicted based on EPA (i) were removed from the
663 EPI. The number and ratio of EPI overlapped with chromatin interactions were counted.
664 Third, EPI were predicted based on EPA (iii), and EPI predicted based on EPA (i) and
665 (ii) were removed from the EPI. The number and ratio of EPI overlapped with
666 chromatin interactions were counted. The number and ratio of the EPI compared two
667 times between EPA (i) and (iii), and EPA (i) and (ii) (binomial distribution, p-value <
668 0.025 for each test).

669 For comparison of EPA with chromatin interactions (HiChIP) in $CD4^+$ T cells,
670 'GSM2705049_Naive_HiChIP_H3K27ac_B2T1_allValidPairs.txt' file was downloaded

671 from Gene Expression Omnibus (GEO) database (GSM2705049). The resolutions of
672 chromatin interaction data and EPI were adjusted to 5kb before their comparison.
673 Chromatin interactions with more than 6,000 and 1,000 counts for each interaction were
674 used in this study.
675

676 **Acknowledgements**

677 The supercomputing resource was provided by Human Genome Center of the Institute
678 of Medical Science at the University of Tokyo. Computations were partially performed
679 on the NIG supercomputer at ROIS National Institute of Genetics. Publication charges
680 for this article were funded by JSPS KAKENHI Grant Number 16K00387. This
681 research was partially supported by the Platform Project for Supporting in Drug
682 Discovery and Life Science Research（Platform for Dynamic Approaches to Living
683 System）from Japan Agency for Medical Research and Development (AMED). This
684 research was partially supported by Development of Fundamental Technologies for
685 Diagnosis and Therapy Based upon Epigenome Analysis from Japan Agency for
686 Medical Research and Development (AMED). This work was partially supported by
687 JST CREST Grant Number JPMJCR15G1, Japan.
688

689 **Figures**

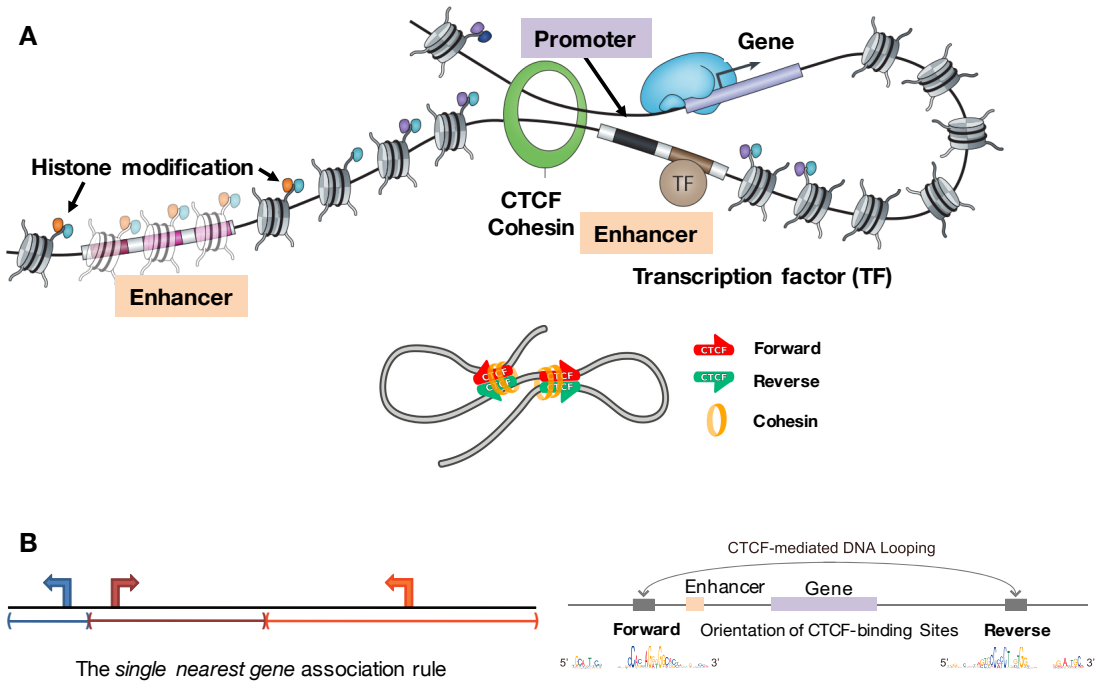

690

691 **Figure 1.** Chromatin interactions and enhancer-promoter association. (A) Forward–
692 reverse orientation of CTCF-binding sites are frequently found in chromatin interaction
693 anchors. CTCF can block the interaction between enhancers and promoters limiting the
694 activity of enhancers to certain functional domains (de Wit et al. 2015; Guo et al. 2015).
695 (B) Computationally-defined regulatory domains for enhancer-promoter association
696 (McLean et al. 2010). The *single nearest gene* association rule extends the regulatory
697 domain to the midpoint between this gene's TSS and the nearest gene's TSS both
698 upstream and downstream. Enhancer-promoter association was shortened at the
699 genomic locations of forward-reverse orientation of DNA binding motif sequence of a
700 transcription factor (e.g. CTCF in the figure).

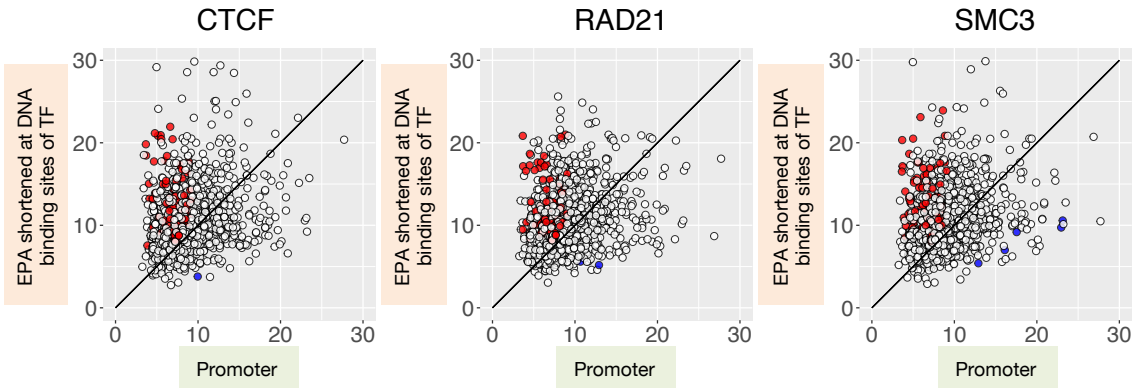

Figure 2. Comparison of expression level of putative transcriptional target genes. The median expression levels of target genes of the same transcription factor binding sequences were compared between promoters and enhancer-promoter association (EPA) shortened at the genomic locations of forward-reverse orientation of DNA motif sequence of CTCF and cohesin (RAD21 and SMC3) respectively in monocytes. Red and blue dots show statistically significant difference (Mann-Whitney test) of the distribution of expression levels of target genes between promoters and the EPA. Red dots show the median expression level of target genes was higher based on the EPA than promoters, and blue dots show the median expression level of target genes was lower based on the EPA than promoters. The expression level of target genes predicted based on the EPA tended to be higher than promoters, implying that transcription factors acted as enhancers of target genes.

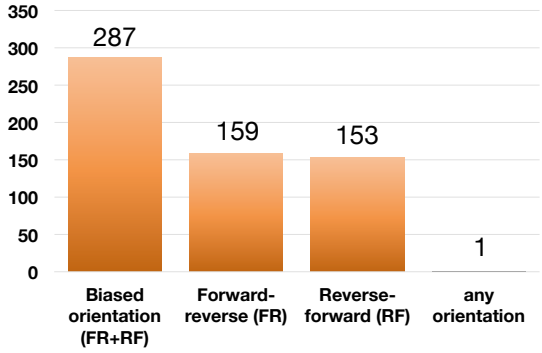

714

715 **Figure 3.** Biased orientation of DNA motif sequences of transcription factors in
716 monocytes. Total 287 of biased orientation of DNA binding motif sequences of
717 transcription factors were found to affect the expression level of putative transcriptional
718 target genes in monocytes of four people in common, whereas only one any orientation
719 (i.e. without considering orientation) of DNA binding motif sequence was found to
720 affect the expression level.

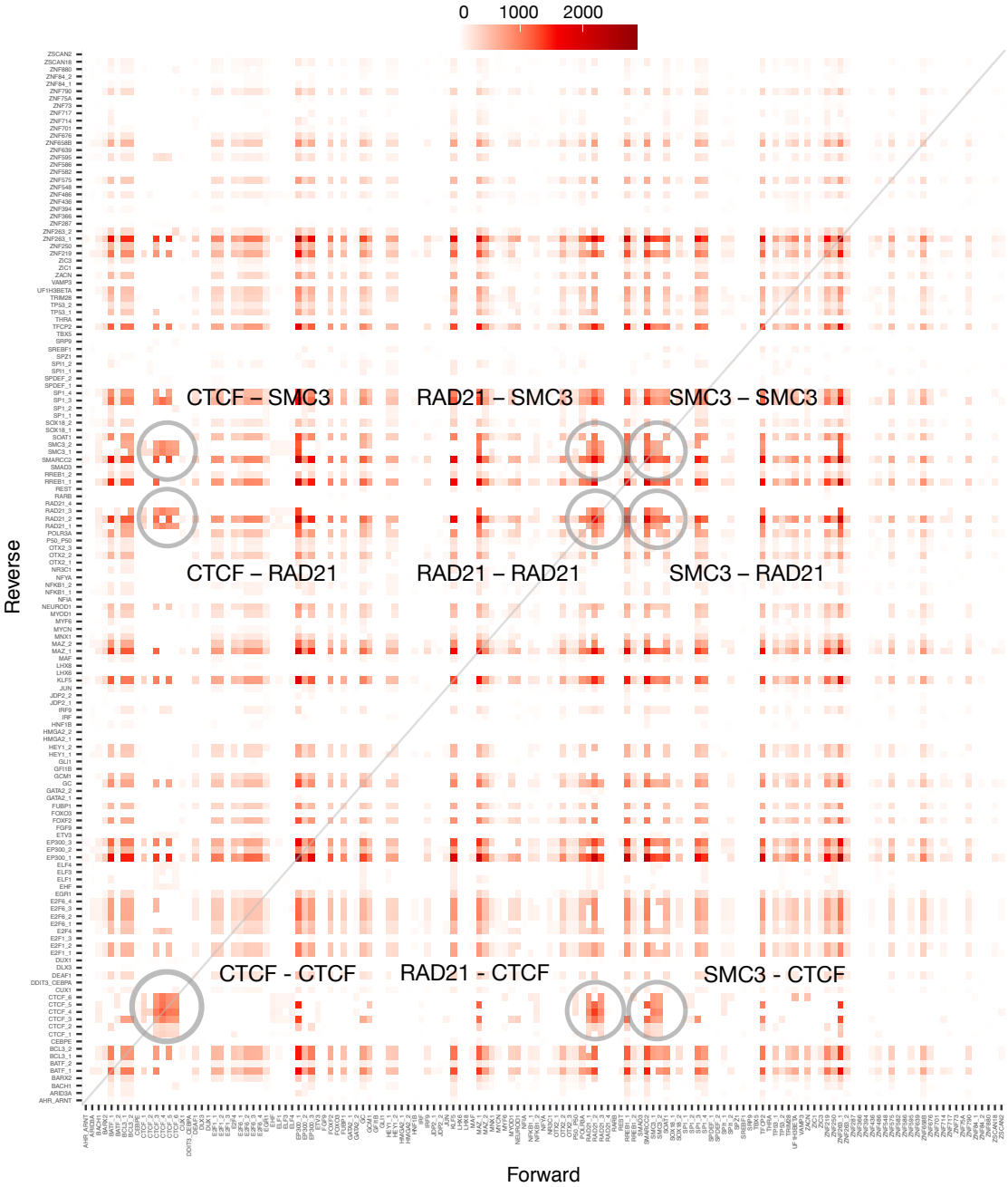

Figure 4. Pairs of biased orientation of DNA binding motif sequences of transcription factors enriched in upstream and downstream of genes. The number of genes with a pair of forward-reverse orientation of DNA motif sequences was counted using all pairs of the DNA motif sequences found in open chromatin regions overlapped with H3K27ac histone modification marks in T cells, and statistical tests (chi-square test) were

727 conducted. The number of genes where a pair of forward-reverse orientation of DNA
728 motif sequences were enriched with p-value < 0.05 was counted and shown as heat map.
729 Gray circles show pairs of DNA motif sequences of CTCF and cohesin (RAD21 and
730 SMC3). CTCF and cohesin are known to be involved in chromatin interactions and
731 have biased orientation of DNA binding motif sequences to form chromatin loops.
732 Other pairs of forward-reverse orientation of DNA motif sequences were also enriched
733 in upstream and downstream of genes.
734

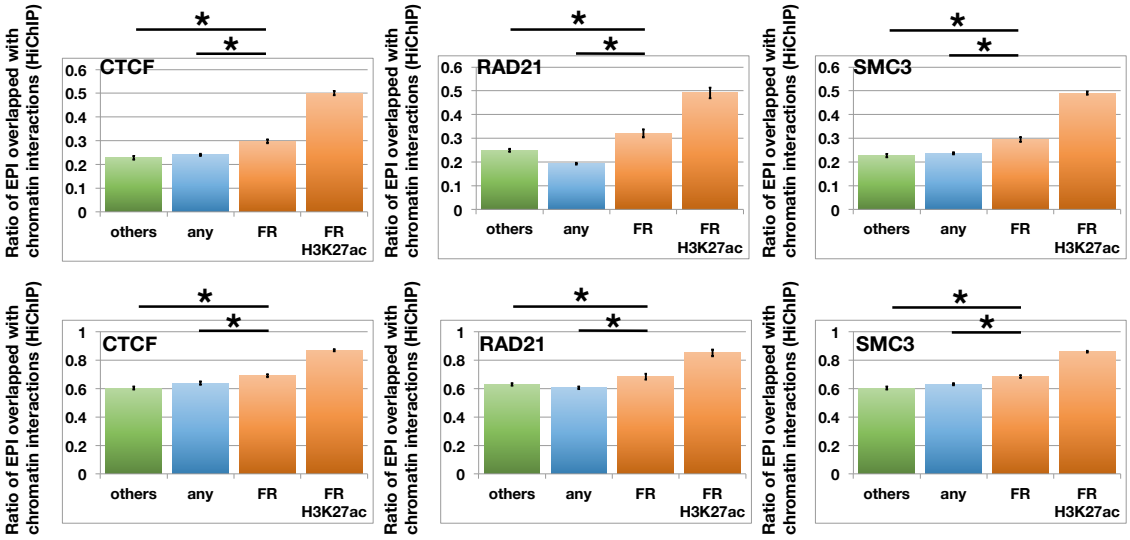

735

736 **Figure 5.** Comparison of enhancer-promoter interactions (EPI) with chromatin
737 interactions in T cells. EPI were predicted based on enhancer-promoter association
738 (EPA) shortened at the genomic locations of biased orientation of DNA binding motif
739 sequence of a transcription factor. Total 121 biased orientation (73 FR and 58 RF) of
740 DNA motif sequences including CTCF and cohesin showed a higher ratio of EPI
741 overlapped with HiChIP chromatin interactions than the other types of EPAs in T cells.
742 The upper part of the figure is a comparison of EPI with HiChIP chromatin interactions
743 with more than 6,000 counts for each interaction, and the lower part of the figure is a
744 comparison of EPI with HiChIP chromatin interactions with more than 1,000 counts for
745 each interaction. FR: forward-reverse orientation of DNA motif. any: any orientation
746 (i.e. without considering orientation) of DNA motif. others: enhancer-promoter
747 association not shortened at the genomic locations of DNA motif. FR H3K27ac: EPI
748 were predicted using DNA motif in open chromatin regions overlapped with H3K27ac
749 histone modification marks. * p-value < 10^{-4}.

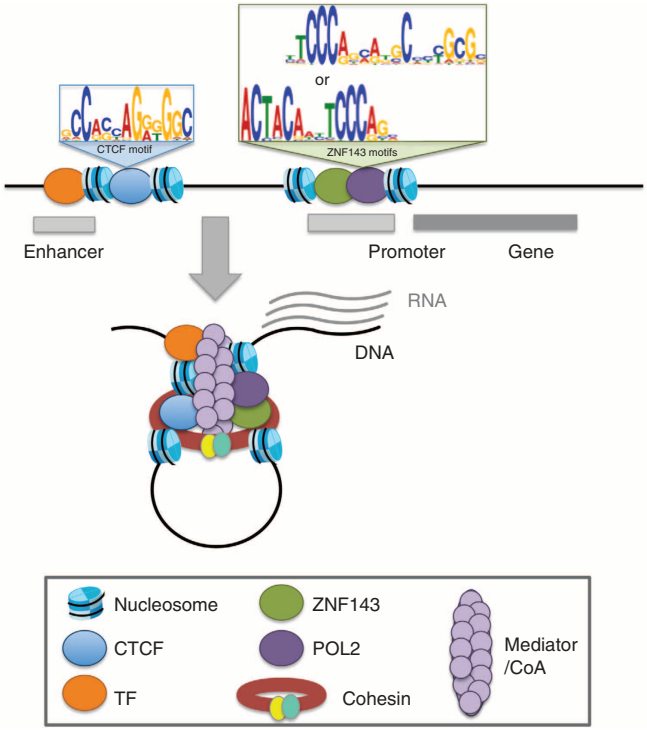

Figure 6. Schematic representation of chromatin interactions involving gene promoters. ZNF143 contributes the formation of chromatin interactions by directly binding the promoter of genes establishing looping with distal element bound by CTCF (Bailey et al. 2015).

Tables

Table 1. Top 90 biased orientation of DNA binding motif sequences of transcription factors in monocytes. TF: DNA binding motif sequences of transcription factors. Score: $-\log_{10}$ (p-value).

Forward-reverse orientation

DNA motif of TF	Score	TF	Score	TF	Score
SRF	75.45	STAT5A	31.24	SMARCC2	21.86
IRF7	71.05	E2F8	30.62	ZNF695	21.78
MINI20	61.68	TP53	30.56	ZNF28	21.77
CTCF	61.62	STAT5B	29.94	ZNF316	21.66
E2F	59.32	STAT3	29.85	TBP	21.60
STAT1	58.94	FOS	29.75	NFIB	21.45
ZNF317	55.97	CEBPZ	29.42	PHOX2B	20.82
CEBPG	55.46	RAD21	28.67	DEC	20.62
ZNF623	54.71	SMAD2	28.60	ZNF709	20.58
ZNF93	54.23	GATA2	28.52	YY1	20.57
HMBOX1	52.99	KLF6	28.02	EIF5A2	20.55
SMAD2_SMAD3_SMAD4	50.66	HOXB1	27.62	ZNF148	20.45
FOXN2	49.88	GLI1	27.09	PAX5	20.05
SPEF1	49.52	GCM1	26.73	POU6F1	19.93
ZNF646	43.95	ZNF676	26.66	FOXO4	19.72
TFE3	42.46	TCF3	26.32	EBF	19.26
MYB	41.98	EHF	26.32	ZNF648	19.12
STAT4	40.54	TCF12	26.29	HENMT1	19.02
ZNF716	40.39	MEF2A	26.22	PARG	18.78
KLF14	39.64	HIC1	25.34	ZNF460	18.64
FOXA1	38.13	EGR2	24.92	SLC25A20	17.83
USF	37.74	NR2F2	24.86	KLF5	17.77
EN1	37.01	PLAGL1	24.65	XRCC4	17.53
ZNF219	35.37	REST	24.53	WT1	17.34
IKZF1	33.79	ZNF143	23.67	SULT1A2	17.34
ZIC1	33.60	YBX1	22.99	FUBP1	17.33
SMC3	33.37	PRDM15	22.63	DNAAF2	17.26
ESR2	32.07	ZNF92	22.22	ZNF521	17.25
TP63	31.98	ZNF214	22.11	XBP1	16.85
ZNF836	31.66	PTF1A	22.09	SP1	16.84

Reverse-forward orientation

TF	Score	TF	Score	TF	Score
RFX5	102.30	TFAP2B	34.55	ZNF449	27.96
TCF7	75.34	TBP	34.47	ZNF233	27.66
SRF	65.52	ZNF670	34.33	SOX2	26.46
ZNF28	63.89	ZNF350	34.30	RXRA	26.07
HNF1B	62.46	ZNF687	33.82	MYF6	25.85
ZNF225	62.18	NFKB2	33.05	MAFK	25.81
CEBPB	59.69	RFX3	32.74	CEBPZ	25.73
NFY	58.96	NFE2L3	32.69	POU2F2	25.59
ZNF286B	54.73	TRIM28	32.27	ETS2	25.05
CTCF	53.16	SP3	32.22	HSF1	24.76
PAX5	52.57	FLI1	32.15	AHR	23.56
STAT1	52.11	RBAK	31.92	PAX6	23.48
ISL1	49.73	NR2F1	31.80	IRF4	22.47
ETV7	47.08	NKX3-1	31.55	ETV3	21.90
KLF16	46.45	ZIC2	31.40	FOXP2	21.72
SP1	46.03	PARP1	31.19	CDX2	21.45
SMAD3	45.27	ZNF195	31.06	NFATC1	21.24
STAT5B	44.72	BDP1	30.84	SP4	21.14
TEAD1	43.00	SOX9	30.72	USF1	20.92
ZNF579	42.94	SP8	30.49	MSX2	20.84
ZBTB2	42.28	ZNF121	30.04	PPARG	20.70
ZNF343	41.01	ZNF202	30.01	MYEF2	20.23
DOBOX5	39.21	CD59	29.85	MYC_MAX	20.22
NANOG	38.84	RXRB	29.57	ZNF711	19.84
NFE2L2	38.53	STAT5A	29.31	ZBTB18	19.60
OBOX2	38.00	SOX11	29.09	HSF2	19.51
ZNF652	37.84	WT1	29.06	DNAAF2	19.00
ZNF30	37.59	CREM	28.65	IRF3	18.88
MYOG	36.34	ZNF316	28.34	TFAP2E	18.87
GABPB1_GABPB2	35.96	HAND1_TCF3	28.07	BCL11A	18.59

Table 2. Top 30 forward-reverse orientation of DNA binding motif sequences of transcription factors in MCF-7 and iPS cells. TF: DNA binding motif sequences of transcription factors. Score: $-\log_{10}$ (p-value).

MCF-7

TF	Score
RAD21	16.21
SMC3	15.63
CTCF	15.12
E2F	10.14
SLC25A20	9.62
HOXA7	8.29
STAT5B	7.55
REST	7.25
SIRT6	7.05
KLF3	6.53
YY1	5.30
PLAGL1	4.97
ZNF219	4.91
STAT1	4.43
SNTB1	4.42
ETS	3.16
XRCC4	3.15
ZBTB6	3.12
DBP	2.53
SETDB1	2.53
RREB1	2.50
E2F5	2.38
KLF5	2.33
SPEF1	2.22
ZNF143	2.20
ZNF460	2.19
FOS	2.18
GATA2	1.97
MAZ	1.95
PARG	1.94

iPS

TF	Score
ZIC3	19.32
ZNF521	18.93
TFE3	16.63
ZNF317	16.43
NKX2-5	16.25
HES1	15.34
ZBTB24	14.21
SMC3	13.76
FOS	13.69
RAD21	13.05
ZNF836	11.64
TBX5	11.48
CTCF	11.24
STAT1	11.19
RUNX2	10.28
WT1	10.27
ZIC1	9.60
MAX	8.55
KLF3	8.29
KLF14	8.25
ZNF143	7.81
E2F5	7.66
SIRT6	7.56
EN1	7.49
YY1	7.02
STAT5B	6.73
MAZ	6.39
ZNF148	6.20
TCF3	5.73
EGR2	5.45

Table 3. Biased orientation of repeat DNA sequences in monocytes. Score: $-\log_{10}$ (p-value).

Forward-reverse (FR) orientation (using H3K27ac histone modification marks)

Repeat DNA seq.	Score
MLT1F1	6.75

Reverse-forward (RF) orientation

Repeat DNA seq.	Score
LTR16C	69.39
L1ME4b	23.90
AluSg	23.61

Table 4. Top 30 of co-locations of biased orientation of DNA binding motif sequences of transcription factors in monocytes. Co-locations of DNA motif sequence of CTCF with another biased orientation of DNA motif sequence were shown in a separate table. Motif 1,2: DNA binding motif sequences of transcription factors. # both: the number of open chromatin regions including both Motif 1 and Motif 2. # motif 1: the number of open chromatin regions including Motif 1. # motif 2: the number of open chromatin regions including Motif 2. # others: the number of open chromatin regions not including Motif 1 and Motif 2. Open chromatin regions overlapped with histone modification marks (H3K27ac) were used (Total 26,095 regions).

Motif 1	Motif 2	# both	# motif 1	# motif 2	# others	*p*-value
CTCF	SMAD2	4527	781	4478	16309	0
CTCF	RREB1	4379	929	4757	16030	0
CTCF	ZNF263	4357	951	4875	15912	0
CTCF	SP1	4321	987	4052	16735	0
CTCF	RAD21	3804	1504	225	20562	0
CTCF	KLF6	3695	852	3800	17748	0
CTCF	SMC3	1259	178	1977	22681	0
CTCF	RXRA	1220	259	2559	22057	0

Motif 1	Motif 2	# both	# motif 1	# motif 2	# others	*p*-value
SMAD2	ZNF263	7427	1578	1805	15285	0
SMARCC2	ZNF263	7354	1192	1893	15656	0
RREB1	SP1	7208	1957	1165	15765	0
SIRT6	ZNF263	7126	1154	2121	15694	0
MAZ	SP1	7052	909	1321	16813	0
MAZ	ZNF263	7022	999	2225	15849	0
SP1	ZNF263	7009	1364	2223	15499	0
SMAD2	SP1	6925	2080	1448	15642	0
MAZ	RREB1	6920	967	2245	15963	0
SIRT6	SMAD2	6766	1514	2239	15576	0
SIRT6	SMARCC2	6668	1612	1878	15937	0
PLAGL1	SMAD2	6637	1074	2368	16016	0
MAZ	SMAD2	6627	1334	2378	15756	0
PARG	SMAD2	6602	1012	2403	16078	0
PLAGL1	ZNF263	6571	1140	2661	15723	0
EGR2	RREB1	6565	787	2600	16143	0
KLF6	RREB1	6563	932	2573	16027	0
MAZ	SMARCC2	6562	1459	1984	16090	0
RREB1	ZNF263	6551	1607	2681	15256	0
KLF6	SP1	6541	954	1832	16768	0
PLAGL1	RREB1	6496	1215	2640	15744	0
EGR2	SP1	6492	860	1881	16862	0
KLF6	SMAD2	6491	1004	2514	16086	0
PARG	ZNF263	6390	1224	2842	15639	0
PLAGL1	SP1	6318	1393	2055	16329	0
KLF6	ZNF263	6304	1191	2928	15672	0
EGR2	SMAD2	6270	1082	2735	16008	0
EGR2	ZNF263	6253	1099	2979	15764	0
EGR2	MAZ	6219	1133	1742	17001	0
PARG	RREB1	6219	1395	2917	15564	0

Table 5. Comparison of enhancer-promoter interactions (EPI) with chromatin interactions in T cells. TF: DNA binding motif sequence of a transcription factor. Score: $-\log_{10}$ (*p*-value). Inf: *p*-value = 0. Score 1: Comparison of EPA shortened at the genomic locations of FR or RF orientation of DNA motif sequence with EPA not shortened. Score 2: Comparison of EPA shortened at the genomic locations of FR or RF orientation of DNA motif sequence with EPA shortened at the genomic locations of any orientation of DNA motif sequence.

Forward-reverse (FR) orientation

TF	Score 1	Score 2
APEX1	13.57	3.85
AR	Inf	8.30
CDC5L	65.46	12.23
CTCF	101.79	14.94
DDIT3_CEBPA	249.72	4.78
EBF1	48.10	2.27
EGR1	97.56	6.09
EGR3	130.86	2.73
EGR4	59.94	2.91
ELF5	119.97	2.85
EP300	28.41	15.12
ETV4	270.06	2.16
FOXF2	42.79	5.16
FOXN4	76.81	4.80
FOXO3	323.31	5.49
FOXO6	63.29	1.77
GATA	104.41	2.17
GATA5	89.03	4.38
GFI1B	184.13	11.81
GLIS2	32.14	1.87
HBP1	281.23	3.05
HIC1	101.63	3.27
HOXA13	103.63	3.71
HOXA2	323.31	5.81
INSM2	323.31	2.02
IRF	206.25	2.09
IRF5	39.54	3.78
KLF1	146.64	3.51
LHX8	245.03	2.34
MAF	66.63	3.85
MINI20	102.68	3.29
MYC	39.24	2.64
MZF1	24.10	1.64
NFATC2	37.81	1.92
NFKB1	195.32	11.43
NR0B1	13.24	1.84
NR2C2	137.27	12.28
OTX2	40.38	2.77
P50_P50	131.79	6.49
PITX1	37.22	2.17

TF	Score 1	Score 2
PRDM15	Inf	3.21
RAD21	56.16	4.21
RARB	113.99	2.28
REL	104.66	7.95
RREB	117.64	3.13
RREB1	116.79	3.39
SMC3	90.56	17.59
SOAT1	22.63	1.88
SOX18	113.13	6.71
SRP9	117.49	3.47
TAL1	70.39	1.82
TCF7L2	93.32	8.22
TFCP2	260.99	4.13
THRA	145.85	4.05
TP53	323.31	9.13
TP63	172.00	3.90
YBX1	164.76	5.23
ZBTB7A	66.49	4.74
ZFP14	97.38	5.25
ZNF219	32.59	7.48
ZNF253	323.31	21.30
ZNF585A	185.37	6.09
ZNF616	129.96	8.66
ZNF639	193.43	1.77
ZNF681	323.31	35.04
ZNF701	41.48	1.65
ZNF721	225.60	5.52
ZNF75A	43.99	3.51
ZNF770	66.18	2.95
ZNF786	323.31	15.68
ZNF790	74.59	6.71
ZNF84	149.37	3.38
ZNF846	Inf	10.92

Reverse-forward (RF) orientation

TF	Score 1	Score 2
BCL11B	101.77	5.58
CEBPA	323.31	2.37
CREB3	139.16	13.51
CTCF	119.43	20.80
DBP	25.72	1.84
EGR1	247.74	1.65
EP300	135.93	6.30
ESR1	101.75	9.30
ETS1	250.92	1.76
ETV1	272.94	3.43
ETV3	323.31	2.99
FOS	101.53	9.02
FOXA	323.31	9.16
FOXA1	323.31	8.99
FOXG1	235.13	2.77
FOXN4	61.07	5.39
FOXO3	306.90	5.33
GATA1	314.93	1.91
HLTF	82.82	1.85
HOXA10	29.26	1.81
HOXB6	197.15	2.21
IRF5	Inf	6.92
KLF13	148.08	4.91
KLF8	120.36	2.97
NFE2L2	155.83	3.83
NFKB1	106.02	7.09
NKX2-1	323.31	4.01
NKX2-4	Inf	5.73
NKX2-5	323.31	5.80
NR4A1	116.75	2.99
PPARGC1A	57.39	3.36
RAD21	41.87	3.16
RUNX2	124.18	5.84
SIX6	95.00	3.28
SMARC	323.31	6.02
SRF	323.31	6.78
TAL1	124.35	4.80
TCF12	74.48	2.21
ZBTB18	240.63	9.05
ZBTB4	323.31	2.06

TF	Score 1	Score 2
ZFP2	323.31	6.24
ZNF143	134.24	1.81
ZNF174	159.72	7.65
ZNF257	172.88	3.75
ZNF28	323.31	3.53
ZNF282	100.44	4.02
ZNF300	Inf	3.91
ZNF341	94.91	5.59
ZNF44	165.34	3.45
ZNF484	301.75	12.63
ZNF526	82.28	4.67
ZNF580	55.73	2.98
ZNF625	323.31	2.31
ZNF658	92.95	4.92
ZNF718	165.94	2.09
ZNF721	86.39	7.28
ZNF773	219.31	13.43
ZNF777	137.69	1.96

798 **References**

799

800 Bailey SD, Zhang X, Desai K, Aid M, Corradin O, Cowper-Sal Lari R, Akhtar-Zaidi B,
801 Scacheri PC, Haibe-Kains B, Lupien M. 2015. ZNF143 provides sequence
802 specificity to secure chromatin interactions at gene promoters. *Nat Commun* **2**:
803 6186.
804 Bailey TL, Boden M, Buske FA, Frith M, Grant CE, Clementi L, Ren J, Li WW, Noble
805 WS. 2009. MEME SUITE: tools for motif discovery and searching. *Nucleic*
806 *acids research* **37**: W202-208.
807 Barutcu AR, Lajoie BR, Fritz AJ, McCord RP, Nickerson JA, van Wijnen AJ, Lian JB,
808 Stein JL, Dekker J, Stein GS et al. 2016. SMARCA4 regulates gene expression
809 and higher-order chromatin structure in proliferating mammary epithelial cells.
810 *Genome research* **26**: 1188-1201.
811 Bejerano G, Lowe CB, Ahituv N, King B, Siepel A, Salama SR, Rubin EM, Kent WJ,
812 Haussler D. 2006. A distal enhancer and an ultraconserved exon are derived
813 from a novel retroposon. *Nature* **441**: 87-90.
814 Chen M, Manley JL. 2009. Mechanisms of alternative splicing regulation: insights from
815 molecular and genomics approaches. *Nat Rev Mol Cell Biol* **10**: 741-754.
816 Das D, Clark TA, Schweitzer A, Yamamoto M, Marr H, Arribere J, Minovitsky S,
817 Poliakov A, Dubchak I, Blume JE et al. 2007. A correlation with exon
818 expression approach to identify cis-regulatory elements for tissue-specific
819 alternative splicing. *Nucleic acids research* **35**: 4845-4857.
820 de Souza FS, Franchini LF, Rubinstein M. 2013. Exaptation of transposable elements
821 into novel cis-regulatory elements: is the evidence always strong? *Mol Biol Evol*
822 **30**: 1239-1251.
823 de Wit E, Vos ES, Holwerda SJ, Valdes-Quezada C, Verstegen MJ, Teunissen H,
824 Splinter E, Wijchers PJ, Krijger PH, de Laat W. 2015. CTCF Binding Polarity
825 Determines Chromatin Looping. *Molecular cell* **60**: 676-684.
826 Grant CE, Bailey TL, Noble WS. 2011. FIMO: scanning for occurrences of a given
827 motif. *Bioinformatics (Oxford, England)* **27**: 1017-1018.
828 Guo Y, Xu Q, Canzio D, Shou J, Li J, Gorkin DU, Jung I, Wu H, Zhai Y, Tang Y et al.
829 2015. CRISPR Inversion of CTCF Sites Alters Genome Topology and

830 Enhancer/Promoter Function. *Cell* **162**: 900-910.
831 Javierre BM, Burren OS, Wilder SP, Kreuzhuber R, Hill SM, Sewitz S, Cairns J,
832 Wingett SW, Varnai C, Thiecke MJ et al. 2016. Lineage-Specific Genome
833 Architecture Links Enhancers and Non-coding Disease Variants to Target Gene
834 Promoters. *Cell* **167**: 1369-1384 e1319.
835 Jeong M, Huang X, Zhang X, Su J, Shamim M, Bochkov I, Reyes J, Jung H, Heikamp
836 E, Presser Aiden A et al. 2017. A Cell Type-Specific Class of Chromatin Loops
837 Anchored at Large DNA Methylation Nadirs. *bioRxiv*.
838 Ji X, Dadon DB, Abraham BJ, Lee TI, Jaenisch R, Bradner JE, Young RA. 2015.
839 Chromatin proteomic profiling reveals novel proteins associated with
840 histone-marked genomic regions. *Proc Natl Acad Sci U S A* **112**: 3841-3846.
841 Jin C, Kato K, Chimura T, Yamasaki T, Nakade K, Murata T, Li H, Pan J, Zhao M, Sun
842 K et al. 2006. Regulation of histone acetylation and nucleosome assembly by
843 transcription factor JDP2. *Nat Struct Mol Biol* **13**: 331-338.
844 Jjingo D, Conley AB, Wang J, Marino-Ramirez L, Lunyak VV, Jordan IK. 2014.
845 Mammalian-wide interspersed repeat (MIR)-derived enhancers and the
846 regulation of human gene expression. *Mob DNA* **5**: 14.
847 John S, Sabo PJ, Thurman RE, Sung MH, Biddie SC, Johnson TA, Hager GL,
848 Stamatoyannopoulos JA. 2011. Chromatin accessibility pre-determines
849 glucocorticoid receptor binding patterns. *Nature genetics* **43**: 264-268.
850 Jolma A, Yan J, Whitington T, Toivonen J, Nitta KR, Rastas P, Morgunova E, Enge M,
851 Taipale M, Wei G et al. 2013. DNA-binding specificities of human transcription
852 factors. *Cell* **152**: 327-339.
853 Karolchik D, Barber GP, Casper J, Clawson H, Cline MS, Diekhans M, Dreszer TR,
854 Fujita PA, Guruvadoo L, Haeussler M et al. 2014. The UCSC Genome Browser
855 database: 2014 update. *Nucleic acids research* **42**: D764-770.
856 Katainen R, Dave K, Pitkanen E, Palin K, Kivioja T, Valimaki N, Gylfe AE, Ristolainen
857 H, Hanninen UA, Cajuso T et al. 2015. CTCF/cohesin-binding sites are
858 frequently mutated in cancer. *Nature genetics* **47**: 818-821.
859 Kheradpour P, Kellis M. 2014. Systematic discovery and characterization of regulatory
860 motifs in ENCODE TF binding experiments. *Nucleic acids research* **42**:
861 2976-2987.
862 Li H, Durbin R. 2009. Fast and accurate short read alignment with Burrows-Wheeler

863 transform. *Bioinformatics (Oxford, England)* **25**: 1754-1760.
864 Li H, Handsaker B, Wysoker A, Fennell T, Ruan J, Homer N, Marth G, Abecasis G,
865 Durbin R, Genome Project Data Processing S. 2009. The Sequence
866 Alignment/Map format and SAMtools. *Bioinformatics (Oxford, England)* **25**:
867 2078-2079.
868 McLean CY, Bristor D, Hiller M, Clarke SL, Schaar BT, Lowe CB, Wenger AM,
869 Bejerano G. 2010. GREAT improves functional interpretation of cis-regulatory
870 regions. *Nature biotechnology* **28**: 495-501.
871 Mumbach MR, Satpathy AT, Boyle EA, Dai C, Gowen BG, Cho SW, Nguyen ML,
872 Rubin AJ, Granja JM, Kazane KR et al. 2017. Enhancer connectome in primary
873 human cells identifies target genes of disease-associated DNA elements. *Nature*
874 *genetics* **49**: 1602-1612.
875 Newburger DE, Bulyk ML. 2009. UniPROBE: an online database of protein binding
876 microarray data on protein-DNA interactions. *Nucleic acids research* **37**:
877 D77-82.
878 Osato N. 2018. Characteristics of functional enrichment and gene expression level of
879 human putative transcriptional target genes. *BMC Genomics* **19**: 957.
880 Phanstiel DH, Van Bortle K, Spacek D, Hess GT, Shamim MS, Machol I, Love MI,
881 Aiden EL, Bassik MC, Snyder MP. 2017. Static and Dynamic DNA Loops form
882 AP-1-Bound Activation Hubs during Macrophage Development. *Molecular cell*
883 **67**: 1037-1048.e1036.
884 Portales-Casamar E, Thongjuea S, Kwon AT, Arenillas D, Zhao X, Valen E, Yusuf D,
885 Lenhard B, Wasserman WW, Sandelin A. 2010. JASPAR 2010: the greatly
886 expanded open-access database of transcription factor binding profiles. *Nucleic*
887 *acids research* **38**: D105-110.
888 Ramani V, Cusanovich DA, Hause RJ, Ma W, Qiu R, Deng X, Blau CA, Disteche CM,
889 Noble WS, Shendure J et al. 2016. Mapping 3D genome architecture through in
890 situ DNase Hi-C. *Nat Protoc* **11**: 2104-2121.
891 Rao SS, Huntley MH, Durand NC, Stamenova EK, Bochkov ID, Robinson JT, Sanborn
892 AL, Machol I, Omer AD, Lander ES et al. 2014. A 3D map of the human
893 genome at kilobase resolution reveals principles of chromatin looping. *Cell* **159**:
894 1665-1680.
895 Rebollo R, Romanish MT, Mager DL. 2012. Transposable elements: an abundant and

896 natural source of regulatory sequences for host genes. *Annu Rev Genet* **46**:
897 21-42.
898 Saeed S, Quintin J, Kerstens HH, Rao NA, Aghajanirefah A, Matarese F, Cheng SC,
899 Ratter J, Berentsen K, van der Ent MA et al. 2014. Epigenetic programming of
900 monocyte-to-macrophage differentiation and trained innate immunity. *Science*
901 *(New York, NY)* **345**: 1251086.
902 Schreiber J, Libbrecht M, Bilmes J, Noble W. 2017. Nucleotide sequence and DNaseI
903 sensitivity are predictive of 3D chromatin architecture. *bioRxiv*.
904 Tabuchi TM, Deplancke B, Osato N, Zhu LJ, Barrasa MI, Harrison MM, Horvitz HR,
905 Walhout AJ, Hagstrom KA. 2011. Chromosome-biased binding and gene
906 regulation by the Caenorhabditis elegans DRM complex. *PLoS Genet* **7**:
907 e1002074.
908 Wang ET, Sandberg R, Luo S, Khrebtukova I, Zhang L, Mayr C, Kingsmore SF,
909 Schroth GP, Burge CB. 2008. Alternative isoform regulation in human tissue
910 transcriptomes. *Nature* **456**: 470-476.
911 Wang J, Vicente-Garcia C, Seruggia D, Molto E, Fernandez-Minan A, Neto A, Lee E,
912 Gomez-Skarmeta JL, Montoliu L, Lunyak VV et al. 2015. MIR retrotransposon
913 sequences provide insulators to the human genome. *Proc Natl Acad Sci U S A*
914 **112**: E4428-4437.
915 Wang L, Wang S, Li W. 2012. RSeQC: quality control of RNA-seq experiments.
916 *Bioinformatics (Oxford, England)* **28**: 2184-2185.
917 Weintraub AS, Li CH, Zamudio AV, Sigova AA, Hannett NM, Day DS, Abraham BJ,
918 Cohen MA, Nabet B, Buckley DL et al. 2017. YY1 Is a Structural Regulator of
919 Enhancer-Promoter Loops. *Cell* **171**: 1573-1588 e1528.
920 Wingender E, Dietze P, Karas H, Knuppel R. 1996. TRANSFAC: a database on
921 transcription factors and their DNA binding sites. *Nucleic acids research* **24**:
922 238-241.
923 Xie Z, Hu S, Blackshaw S, Zhu H, Qian J. 2010. hPDI: a database of experimental
924 human protein-DNA interactions. *Bioinformatics (Oxford, England)* **26**:
925 287-289.
926 Zhang H, Li F, Jia Y, Xu B, Zhang Y, Li X, Zhang Z. 2017. Characteristic arrangement
927 of nucleosomes is predictive of chromatin interactions at kilobase resolution.
928 *Nucleic acids research* **45**: 12739-12751.

Zhang Y, An L, Xu J, Zhang B, Zheng WJ, Hu M, Tang J, Yue F. 2018. Enhancing Hi-C data resolution with deep convolutional neural network HiCPlus. *Nat Commun* **9**: 750.

Zhao Y, Stormo GD. 2011. Quantitative analysis demonstrates most transcription factors require only simple models of specificity. *Nature biotechnology* **29**: 480-483.